AIAA JOURNAL
Vol. 51, No. 5, May 2013

Intermittent Nature of Subsonic Jet Noise

M. Kearney-Fischer,* A. Sinha,† and M. Samimy‡
Ohio State University, Columbus, Ohio 43235-7531

DOI: 10.2514/1.J051930

Following on previous works showing that far-field jet noise has significant intermittent aspects, the present work assumes that these intermittent events are the dominant feature of jet noise. A definition and method of detection for intermittent noise events is devised and implemented. Using a large experimental database of acoustically subsonic jets with different jet acoustic Mach numbers ($M_a = 0.5$–0.9), nozzle diameters ($D = 2.54, 5.08,$ and 7.62 cm), and jet exit temperature ratios (0.84–2.70), these events are extracted from the far-field noise signals measured in the anechoic chamber of the NASA Glenn Aero-Acoustic Propulsion Laboratory. It is shown that a signal containing only these intermittent events retains all of the important aspects of the acoustic spectrum for jet noise radiating to aft angles, validating the assumption that intermittent events are the dominant feature of aft angle jet noise. Statistical analysis of the characteristics of these noise events reveals that these events can be described in terms of three parameters (the variance of the original signal, the mean width of the events, and the mean time between events) and two universal statistical-distribution curves. The variation of these parameters with noise-radiation direction, nozzle diameter, and jet velocity and temperature are discussed. There is a strong correlation between the mean width of the intermittent events and the mean time between the events ($\overline{\delta t}/\overline{\Delta T} = 0.128 \pm 0.002$) in all the cases investigated in this work, implying a strong link between dynamics governing the two quantities.

Nomenclature

A_i	=	ith event amplitude, Pa
a_∞	=	ambient speed of sound, m/s
D	=	jet exit diameter, cm
He	=	$f \cdot D/a_\infty$, Helmholtz number
ℓ	=	shape parameter of the gamma distribution
M_a	=	U_j/a_∞, jet acoustic Mach number
p	=	far-field acoustic pressure, Pa
p_{RMS}	=	root mean square pressure, Pa
St_D	=	$f \cdot D/U$, Strouhal number
T_i	=	ith event temporal coordinate, s
U_j	=	jet exit velocity, m/s
$\overline{\Delta T}$	=	mean event intermittence, ms
$\overline{\delta t}$	=	mean event width, μs
δt_i	=	ith event width, μs
ξ	=	scale parameter of the gamma distribution, μs
σ	=	standard deviation parameter of normal distribution, Pa
τ_∞	=	inverse Helmholtz number
τ_j	=	inverse Strouhal number
ϕ	=	jet polar angle relative to downstream axis, deg

I. Introduction

JET noise is a problem that has plagued the use of jet engines since their inception. Despite more than six decades of research since the seminal work of Lighthill [1], a clear picture of jet-noise sources has not yet emerged [2]. Part of the problem is the sheer number of jet operating parameters that have been shown to impact jet-noise production (temperature, pressure, density, hydrodynamic Mach number, acoustic Mach number, nozzle geometry, exit boundary layer state and turbulence level, etc.). Many of these parameters are interrelated, and no unified standard exists for reducing them to the minimum set of independent parameters; this leads to additional confusion about overlapping experimental regimes. Although there have been advances in empirically based models [3,4] and theoretical analysis [5] of jet noise, the essential features of jet noise are still debated. Without a reasonably simple model incorporating the essential features of jet noise, understanding of their sources is clearly impeded.

There have been two dominant methods of experimental data analysis in jet aeroacoustics: 1) Fourier spectrum analysis, and 2) correlation analysis. Spectral analysis is the fundamental tool used by the aeroacoustics community, and for good reason. Spectral analysis discards temporal information making it impossible to link particular aspects of the frequency domain back to segments of the signal in time. Correlation analysis provides links between two signals in time, but only if their trends are sufficiently similar; it can indicate how similar the trends of two signals are and how the similarity is displaced in time. These two tools have provided researchers with a wealth of information and insight, but with certain restrictions.

Using additional tools that are designed for temporally compact fluctuations has the potential to contribute new aspects of understanding. Relatively recently, tools like the wavelet transform have been used to obtain a different perspective of the noise signal. The basic theme of these works is the supposition that acoustically subsonic jet noise (at least in the radiation to aft angles) is made up of intermittent bursts as opposed to continuous variations. Understanding this kind of signal requires a different analysis methodology from what has been prevalent in the literature. In a previous work from the Gas Dynamics and Turbulence Laboratory (GDTL) of the Ohio State University, Hileman et al. [6] showed that, if the amplitudes of the intermittent bursts (in this context, defined as portions of the signal that exceeded twice the root mean square pressure, 2 p_{RMS}) were reduced by 50%, the peak region of the spectrum was reduced by about 4 dB. Hileman et al. used the assumption that the bursts are a significant constituent of the noise

Presented as Paper 2012-1167 at the 50th AIAA Aerospace Sciences Meeting, Nashville, TN, 9–12 January 2012; received 1 April 2012; revision received 1 December 2012; accepted for publication 5 December 2012; published online 15 March 2013.

*Graduate Research Associate, Department of Mechanical and Aerospace Engineering, Gas Dynamics and Turbulence Laboratory, Aeronautical and Astronautical Research Laboratories, 2300 West Case Road; currently Senior Aeronautical Engineer, Lockheed Martin Advanced Development Programs, Palmdale, CA 93599.

†Graduate Research Associate, Department of Mechanical and Aerospace Engineering, Gas Dynamics and Turbulence Laboratory, Aeronautical and Astronautical Research Laboratories, 2300 West Case Road; currently Postdoctoral Researcher, Department of Mechanical and Civil Engineering, California Institute of Technology, Pasadena, CA 91106.

‡John B. Nordholt Professor, Department of Mechanical and Aerospace Engineering, Gas Dynamics and Turbulence Laboratory, Aeronautical and Astronautical Research Laboratories, 2300 West Case Road; Samimy.1@osu.edu. Fellow AIAA (Corresponding Author).

signal, but not necessarily the primary feature. The purpose of the present paper is to take this previous assumption to its extreme limit: assume that these bursts (hereafter referred to as noise "events") are the dominant feature of jet noise. The paper is divided as follows:

1) A noise event as well as a method of its identification and characterization is defined and discussed.

2) The spectrum of the events-only signal p_e is computed and compared to the total signal.

3) Statistical analysis of these events is performed for an extensive experimental data set.

4) The implications of the statistical analysis on jet-noise-source models are discussed.

II. Background

Fourier spectrum analysis is a powerful tool used throughout the scientific world for signal analysis of all kinds. This approach has contributed to many of the currently understood aspects of jet noise including, but not limited to: directivity, scaling with size and velocity, and identification of different types of noise sources. Consequently, this tool is a staple of the aeroacoustics community and a benchmark for any new theory or analysis technique. One example using spectral analysis is Viswanathan's work on scaling [4] that incorporates temperature and directivity effects into an empirical model. Another example of the power of spectral analysis is Tam's two noise-source model [3,7], which proposes that the mixing noise in jets can be described by two types of source spectra that are superposed with different weights at different polar angles.

Correlation analysis is another powerful tool that has contributed to many of the same areas of understanding of jet noise as spectral analysis [e.g., 8–11]. Studies using this tool are looking for relationships between different variables (e.g., velocity and density) or the same variables but at different regions of interest in a flow (e.g., near-field to far-field or flow-field to far-field). Typically, signals from different points in space are correlated to look at the relationships between those locations in terms of propagation or directivity. Many of these studies use correlation analysis to locate noise sources in space and/or time in an attempt to link the result (i.e., acoustic radiation) back to the cause (i.e., the turbulent dynamics that produce the noise).

The papers cited previously are but a few examples of the enormous body of work that has been generated in the decades of research on jet noise. For many hundreds more examples of works using these tools in the pursuit of understanding jet noise, the reader is referred to any of the several review papers that have been written on the subject [2,12–15].

Fourier analysis uses oscillating signals with infinite extent and describes the examined signal in terms of those oscillations. Therefore, it is not optimized for characterizing localized events. It should be remembered that, because of the nature of the Fourier transform, all of the information in the signal is preserved in some fashion when a signal is transformed; it may just be very difficult to identify from the spectrum. Using a tool that examines the signal in a different way may provide more efficient access to particular kinds of information that may be beneficial in improving the understanding of the signal.

A few researchers have chosen to examine (and/or use) the intermittent nature of the signal in analysis of the acoustic far-field (e.g., [6,16–24]). A common theme that unifies these works is the use of wavelet analysis, the underlying principle of which is that the signals under examination cannot be adequately described by a set of periodic waves.

In the case of the previous works from Heileman et al. [6] and Kastner et al. [16], the intermittence in the far-field noise provides a basis for a source-localization method. A wavelet transform of the far-field signal showed that there were spikes in the signal. Based on this observation, noise events were defined as spikes rising above a specified threshold in the time domain. The localization method used a microphone array and the times of arrival at the various microphones of these spikes to locate the source of an event in space–time. As discussed in those works, the calculated region of noise sources agrees with other research, indicating that the noise radiated at aft angles (~30 deg) comes from an area near the end of the potential core. Simultaneous flow visualizations using a megahertz-rate imaging system showed that these events are associated with dynamically significant behavior of the large-scale structures. It was also shown that, when the amplitude of these statistically outlying events was artificially reduced via signal postprocessing, the amplitude of the spectral peak could be reduced by several decibels. Guj et al. [21] used a similar kind of conditional averaging of the flow-field to determine that bursts of noise were related to dynamically significant fluctuations of the large-scale structures.

Cavalieri et al. [18] look at the direct numerical simulations of an uncontrolled and an optimally noise-controlled two-dimensional mixing layer of Wei and Freund [25]. They show that the optimally controlled case accomplishes noise reduction by suppressing certain intermittent peaks in the signal, highlighting the need to include intermittency in sound prediction schemes. Noise suppression in this simulation was related to preventing the merger of three vortices (a triple merger) that was shown to produce a large spike in the acoustic signal. Cavalieri et al. [19] discuss a wave-packet model in which the envelope function varies in both space and time. This analysis, which follows the idea originally suggested by Kastner et al. [26], shows that a high-amplitude event (i.e., a pressure spike) can be produced when the wave-packet is truncated by fluctuations in the envelope. Grassucci et al. [17] use a wavelet domain filter to separate near-field pressure fluctuations into intermittent and nonintermittent signals. They then relate the intermittent signal to velocity fluctuations in the jet using linear stochastic estimation. Although this work is preliminary, their initial results are promising. Grizzi and Camussi [24] use wavelet transforms to separate the acoustic and hydrodynamic fluctuations in near-field pressure data. Koenig et al. [20,27,28] have started using wavelet transforms and filtering in the wavelet domain to isolate these intermittent events for study. This analysis uses a fourth-order Paul wavelet to decompose the signals with a continuous wavelet transform. Results to date have mainly focused on the relationship of the resulting directivity patterns to wave-packet models for jet noise. One observation in Koenig et al. [27] is that using Helmholtz number can achieve better spectral collapse for varying acoustic Mach number than Strouhal number scaling in unheated jets. This scaling with Helmholtz number has also been seen by other researchers [29] and is further discussed in Sec. VI. Low et al. [23] use wavelet filtering and correlation on both near and far-field to determine how the near-field events are related to the far-field events. Their work is still preliminary but warrants mentioning as a significant attempt to trace the intermittent aspects of jet noise back toward their sources.

These works show that jet noise does indeed contain intermittent events and that these events play a significant role in the overall acoustic picture of the jet. The results to date, however, are quite limited in their description of these intermittent events. Issues such as the importance of these events to the total signal spectra, many aspects of the nature of these events (lifetimes, frequency of occurrence, etc.), and the exact relationship of these events to the flow-field dynamics remain to be determined.

III. Noise-Event Definition and Signal Extraction

The hypothesis of this analysis is as follows. The primary noise sources in a mixing-noise-dominated jet (i.e., acoustically subsonic) that radiate to aft angles are intermittent events with periods of relative silence in between. Therefore, a postprocessing routine that highlights these events while suppressing other signal components can shed light on the dynamics of jet noise related to the most-energetic frequencies. Although some of the previous work of other researchers lends support to this premise, only the work of Koenig et al. (see [27] and others) has made the assertion that these events constitute the dominant mechanism of jet-mixing noise. The validity of this premise will be investigated once the analysis process has been explained.

In the absence of a theoretical basis, an ad hoc definition of an event is required. In this analysis, an event is defined as a portion of the signal whose peak exceeds $\pm 1.5 p_{\mathrm{RMS}}$, where the RMS pressure is a unique value for every microphone (dictated by its position in the acoustic field) and jet operating condition. This definition is chosen,

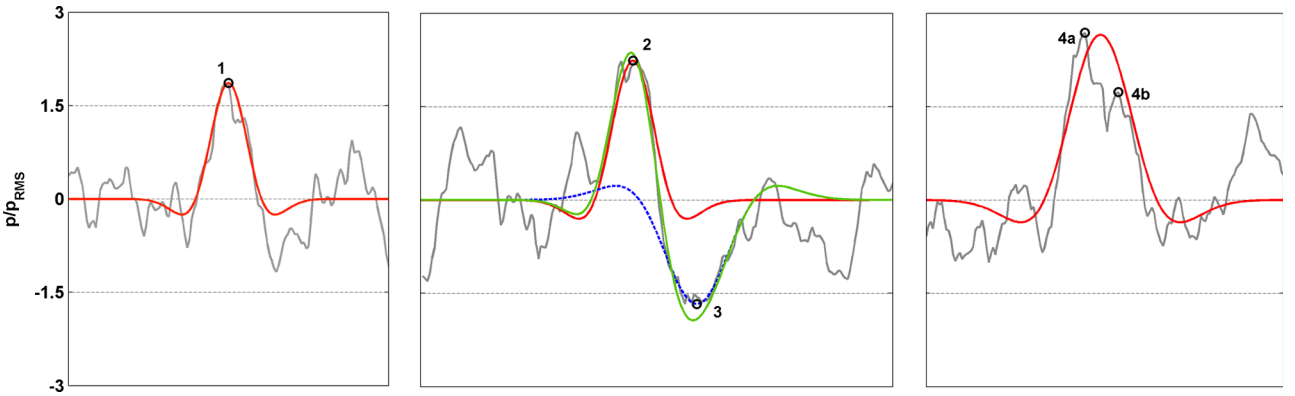

Fig. 1 Examples of the data-reconstruction process (the green curve shows the final waveform from the superposition of events 2 and 3).

in part, because it is consistent with the previous work at the GDTL [6,16]. Other multiples of p_{RMS} were explored, and it was found that 1.5 was the highest threshold that sufficiently reproduced the important spectral characteristics (see Sec. V). The distribution of amplitudes in a far-field noise signal, once normalized by its p_{RMS}, is the *unit* normal distribution (this is demonstrated in Sec. VI.A). Based on the characteristics of the unit normal distribution, this definition ignores about 87% of the signal time. It is important to note that this threshold is unique for every signal. This selection criterion means that noise events are outliers with respect to the total signal in which they exist, and this definition is self-consistent across any signal examined. A selection criterion based on a fixed threshold (either for the entire range of polar angles or based on a particular operating condition) would impose a definition that obviously would be incapable of accounting for scaling.

Examples of the data-extraction and modeling process for the basic types of encountered events are shown in Fig. 1. As discussed in more detail in Sec. V, the events in the figure are modeled with a Mexican hat-type function. It should be understood that the model function has no impact on the data-extraction process; the information extracted is only used with the model function for the purposes of the signal reconstruction for spectral analysis. The fluctuations in the examples are typical, showing the prominence of the fluctuations that are identified as events in comparison to the total signal. For a larger sense of the reconstructed signal, see Fig. 2. Information on the events is extracted as follows:

1) Any contiguous set of points that exceeds the threshold ($\pm 1.5 p_{\mathrm{RMS}}$) is identified as an event; this identifies five regions in the examples (1, 2, 3, 4a, and 4b).

2) For every event i, the peak amplitude A_i and temporal location T_i are identified.

3) The width of an event (i.e., its extent in time, δt_i), defined as the full width at half-maximum (FWHM), is found by scanning outward in both directions from a given peak for the first occurrence of that criterion.

4) A check is performed to look for event overlap: events 4a and 4b in the examples. If the temporal extent of two or more peaks of the same sign overlaps, these events are merged into a single peak with the following properties: width (determined as the time between the left edge of the earliest peak and the right edge of the latest peak — time increasing from left to right — using the half-maximum criterion from the individual peaks); peak location (determined as halfway between the newly determined beginning and end of the merged peak); and peak amplitude (the greatest amplitude in the merged event).

It should be noted that event location and width are determined to single-sample accuracy of the discretely sampled acoustic signal and are not interpolated to a higher precision. One consequence of this data-extraction method is that the minimum event width allowed is three samples. Any subsequent analysis of these quantities will also be quantized at single-sample accuracy. In Sec. VI, these quantities are used to develop a statistical picture of the typical event characteristics.

IV. Experimental Database

The experimental database for this analysis is taken from the Small Hot Jet Acoustic Rig (SHJAR) at the NASA Aero-Acoustic Propulsion Laboratory. This database, taken from a large facility

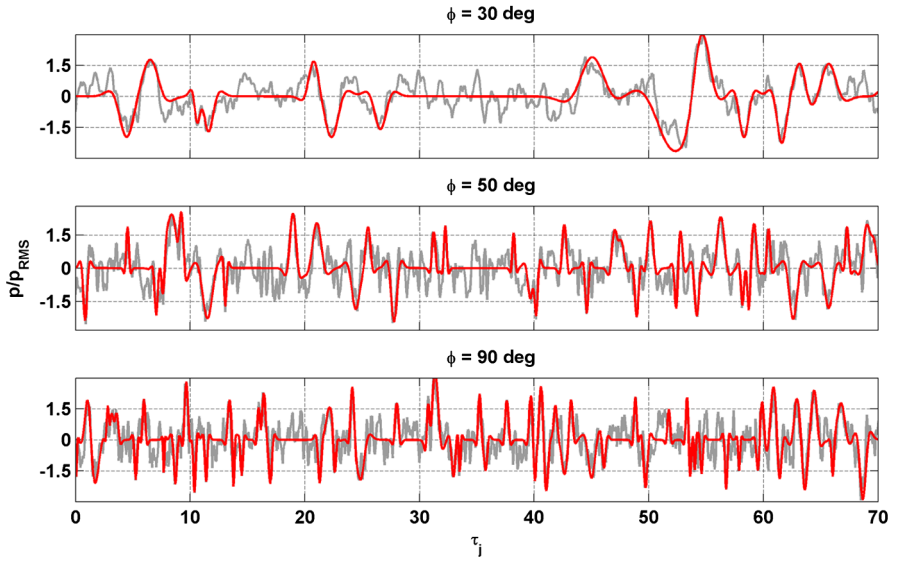

Fig. 2 Time domain of a portion of data for case 5 ($D = 2.54$ cm, TTR $= 1.0$, and $M_a = 0.9$) at three polar angles ($\phi = 30, 50$, and 90 deg) showing the raw data (gray) and the reconstructed signal (red).

Table 1 Experimental operating conditions

D, cm	TTR[a]	M_a	ETR[b]	Case number
2.54	1.00	0.5, 0.6, 0.7, 0.8, 0.9	0.95, 0.93, 0.90, 0.87, 0.84	1–5
5.08	1.00	0.5, 0.6, 0.7, 0.8, 0.9	0.95, 0.93, 0.90, 0.87, 0.84	6–10
5.08	1.81, 1.92	0.5, 0.9	1.76	16–17
5.08	2.31, 2.43	0.5, 0.9	2.27	18–19
5.08	2.75, 2.84	0.5, 0.9	2.70	20–21
7.62	1.00	0.5, 0.6, 0.7, 0.8, 0.9	0.95, 0.93, 0.90, 0.87, 0.84	11–15

[a]Total temperature ratio.
[b]Exit temperature ratio.

validation database study [30,31], is designed to efficiently and effectively explore the various parameters that can affect subsonic jet noise. There are a total of 21 cases covering three jet diameters, five acoustic Mach numbers, and unheated as well as three elevated temperatures. All three of the nozzles in these experiments are axisymmetric. The "case number" will be used later in the paper to refer to the different combinations of nozzle and operating conditions. The total temperature ratio (TTR) is the ratio of the jet stagnation temperature to the ambient temperature, and the exit temperature ratio (ETR) is the ratio the jet exit temperature to the ambient temperature. The exact values of these parameters are enumerated in Table 1. Unless stated otherwise, the Mach number referred to when discussing the data is the acoustic Mach number ($M_a = U_j/a_\infty$).

The SHJAR is housed in a fully anechoic geodesic dome (60 ft radius, 18.3 m) that uses 24 in. (61 cm) long fiberglass wedges to eliminate reflections at all frequencies above 200 Hz. Compressed air (up to 150 psia, 1.03 MPa) is routed through a hydrogen gas combustor, a muffler, a settling chamber, and then a reducer and nozzle, where it is exhausted through a large door to the ambient environment. The combustor produces tones as well as broadband combustion noise that complicate data analysis because they are not fully eliminated by the muffler. The facility can support flow rates up to 6 lbm/s (2.72 kg/s) with stagnation temperatures up to 1300°F (704°C). This facility has 24 microphones on a constant-radius arc ranging from 15 to 130 deg relative to the jet downstream axis spaced every 5 deg. The arc radius is 100 in. (2.54 m) from the nozzle exit for the 1 in. (2.54 cm) and 2 in. (5.08 cm) nozzles and 150 in. (3.81 m) for the 3 in. (7.62 cm) nozzle to ensure that microphones are in the acoustic far-field. All microphones are arranged for normal incidence on stands designed to minimize reflections. Data at this facility are acquired using Bruel and Kjaer model 4939 microphones and Nexus 2690 amplifiers connected using 100 m cables. The outputs of the amplifiers are acquired at 200 kHz and low-pass-filtered at 90 kHz by a DataMAX Instrumentation Recorder from R.C. Electronics Inc. About 8 s of data are acquired for each case. Ambient conditions are monitored in real time to ensure that the properties like acoustic Mach number and ETR can be maintained. Many details such as the nozzle design and validation of the facility are available in [30,31].

V. Spectral Analysis

Before proceeding any further, it is important to determine if the proposed definition of an event has any merit (i.e., whether it captures the important aspects of the signal). Given that spectral analysis is the standard tool of research on jet noise, it would be useful to compare the spectrum of the original signal to one that contains only the high-amplitude events. If, alternatively, the raw signal was simply truncated, in other words if $p(|p| < 1.5p_{\mathrm{RMS}})$) were set to zero, it would introduce a lot of high-frequency content from the sharp corners at the edges of an event. Given that the event locations, amplitudes, and widths are known, it is relatively easy to reconstruct an events-only signal p_e with the appropriate choice of a model function. The model function chosen for this reconstruction is a Mexican hat function:

$$\psi_i(t) = A_i\left(1 - \frac{(t-T_i)^2}{(\delta t_i \epsilon)^2}\right)\exp\left[\frac{-(t-T_i)^2}{(\delta t_i \epsilon)^2}\right] \tag{1}$$

where A_i is the peak amplitude, δt_i is the event width (i.e., FWHM), T_i is the temporal location of the event peak, and ϵ is an adjustment factor that modifies the function so that the FWHM can be used as the characteristic scale. It can be mathematically determined that a correction of 10% is needed to adjust the function to obtain the desired behavior (i.e., $\delta t_{\mathrm{MH}} = 0.9\delta t_i$). Therefore, $\epsilon = 0.9$ was set as a constant for all data processing. The examples in Fig. 1 demonstrate the fitting process. This model function was chosen because of its flexibility. If the true nature of a noise event is a single peak in isolation (event 1 in the examples), this function will probably fit it well unless it is highly asymmetric. If, however, the true nature of a noise event is more complex (i.e., involving multiple positive and negative swings such as the combined structure of events 2 and 3 in the examples), guessing an appropriate universal model function at this point is essentially impossible. Under the current definition, each positive and negative peak in a multiple-swing event will be identified as a separate event and their parameters stored independently. When the events-only signal p_e is reconstructed, the different pieces will be modeled as independent instances of the Mexican hat function. Because this function is amenable to superposition (hence its common use as a wavelet), it should do a good job of representing a more complex shape (see example events 2 and 3). Once the reconstructed signal p_e is calculated, it can be put through the same postprocessing steps as the raw data for calculating the spectrum.

An example of the signal reconstruction is shown in Fig. 2 for three polar angles ($\phi = 30$, 50, and 90 deg). The abscissa is a nondimensionalized time $\tau_j = tD/U_j = 1/St_D$ (inverse Strouhal number), where U_j is the jet exit velocity. The reconstruction does a good job, especially at the aft angles, of reproducing the major aspects of the signal. At aft angles, the time domain is characterized by large, slowly oscillating shapes. As the polar angle increases, the signals become quite jittery (i.e., characterized by rapid oscillations on the order of the sampling resolution). The implications of these different characteristics are further discussed in Sec. VI.

The sound-pressure-level (SPL) spectra for the raw data and reconstructed data at two polar angles ($\phi = 30$ and 90 deg) are shown in Fig. 3 for two disparate jets and operating conditions. It is clear that, especially in the case of 30 deg, the reconstructed signal does a very good job of reproducing the important features of the spectrum (i.e., the peak location and amplitude and the shape of the spectral peak). The decreased high-frequency content is expected because the reconstruction ignores the high-frequency content of the signal except for that which is imposed by the width of events. There is also an increase in the low frequencies due to the basic spectral behavior of the model function, which has a flat spectrum below a characteristic frequency ($f \approx 0.048/\epsilon\delta t$) to represent the localized pulse. The higher angles (90 deg being the representative sample) are fairly well reproduced, but the spectral amplitudes are slightly overpredicted. It is worth noting that no corrections have been applied to these spectra. In typical spectral analysis, a microphone free-field correction, a distance scaling correction, and an atmospheric absorption correction are applied to the calculated spectrum. It was found that the frequency-dependent corrections, which have significant effect only at high frequencies, do not meaningfully alter the characteristics of the signal relevant to this analysis. Additionally, because the definition and subsequent analysis are in terms of p_{RMS}, it is not necessary to scale the data to a standard distance.

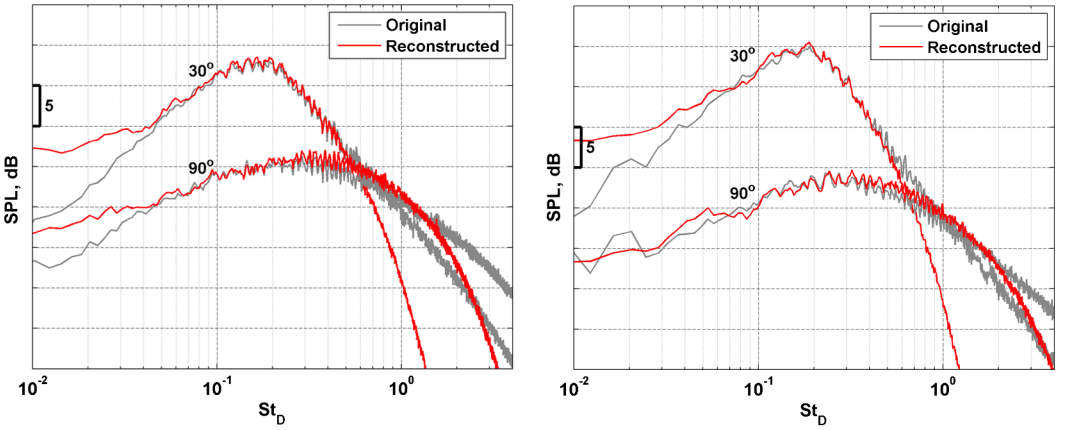

a) D = 2.54 cm, TTR = 1.00, M_a = 0.9 b) D = 5.08 cm, TTR = 2.84, M_a = 0.9

Fig. 3 Example spectra for signal reconstruction.

Some additional information can be gleaned at this point by looking at the energy of the reconstructed signal (E_R = variance[p_e]) compared to the original (E). The ratio of E_R/E is found to be essentially unity. Examining the various polar angles, it is found that this ratio has a range of 1 ± 0.025. This near or slightly over unity reconstruction occurs because the smooth function used to model the events ends up adding some energy at low frequencies (as already discussed), which makes up for the energy eliminated from the high frequencies.

Although there are many cases and polar angles that are not shown, these results are typical for all the cases studied. The aft angles are well predicted by the events-only signal p_e. The sideline and upstream angles are decently represented, but with the spectral amplitudes being a bit overpredicted. Without any additional analysis, these observations provide some important insights.

1) This combination of event definition, data extraction, and signal reconstruction is capturing the vital aspects of jet noise using a simple set of equations and a model function with three parameters: the event amplitude A_i, the event width δt_i, and the event temporal coordinate T_i. This result is expected because most of the signal energy is contained in the large fluctuations that are being captured by this analysis. It can therefore be concluded that acoustically subsonic jet noise (at least for the aft angles) is indeed well described by a fundamentally intermittent signal populated by localized events.

2) As will be further quantified in Sec. VI, the educed noise events in these directions seem to have widths influenced by the sampling rate of the signal (i.e., the oscillations are too fast to be well resolved in the raw data).

3) Based on the two preceding observations, it is concluded that the hypothesis is correct for aft angles. The exact nature of these signals will be quantified by further analysis in Sec. VI.

VI. Statistical Analysis of Events

Using the large number of events captured in a given data set for each polar angle (between 10,000 and 100,000 events, depending on polar angle), it is possible to construct statistical distributions for the various quantities extracted from the data. The purpose of this section is to explore the nature of these extracted quantities through statistical analysis to determine how these quantities scale with jet diameter and operating conditions. In most of this section, analysis will be focused on 30 and 90 deg as representative of the two characteristic types of noise signals found in the subsonic jet.

At this point, it is prudent to briefly describe two statistical-distribution functions that will be used several times in the subsequent analysis. The normal (or Gaussian) distribution is very common and describes quantities that fall symmetrically about some mean; the standard deviation σ will be discussed. The other distribution of note is the gamma distribution that arises from Poisson processes. In a Poisson process, the occurrences of events of interest are independent from one another, and so these occurrences (e.g., wait times) are distributed randomly about some mean where ℓ and ξ are known as the shape and scale parameters, respectively. A few of the relevant properties of the gamma distribution are: 1) the mean occurs at $x = \ell \xi$, 2) the mode occurs at $x = (\ell - 1)\xi$, and 3) the variance of the distribution is $\ell\, \xi^2$.

To look at the scaling properties of these statistics as well as their relationship to the spectra, there are a few quantities that will need to be defined. The first is a nondimensionalized time τ. As seen in Eq. (2), time is nondimensionalized using the jet diameter and either the jet exit velocity (resulting in a quantity that can be thought of as an inverse Strouhal number as already defined in Sec. V) or the ambient speed of sound (in which case the quantity is an inverse Helmholtz number):

$$\tau_j = t\frac{U_j}{D} = \frac{1}{St_D} \qquad \tau_\infty = t\frac{a_\infty}{D} = \frac{1}{He} \tag{2}$$

A. Amplitude Distributions

To analyze the distribution of the event peaks A_i, the signal is quantized into 1000 amplitudes, normalized by the p_{RMS} of that particular signal, and the probability density function (PDF) is computed. In Fig. 4a, the PDF of the signal from the 30 deg microphone is shown for all cases; there are 21 curves of different colors in the figure. It is clear that, once normalized by p_{RMS}, the distribution of amplitudes collapses onto a single curve regardless of the jet size and operating conditions. The unit normal distribution curve is shown in Fig. 4a as a black line. In Fig. 4b, the PDF of the signal from all 24 microphones is shown for one jet with one operating condition along with the unit normal distribution curve. Again, total collapse is achieved. Although it is not possible to observe this from Fig. 4a as rendered, it is found that lower-velocity jets have greater scatter about the unit normal curve, whereas higher-velocity jets, such as the one shown in Fig. 4b, very closely match the unit normal distribution. This change in scatter is true regardless of the jet diameter and temperature. It can therefore be concluded that the distribution of amplitudes in any acoustic signal examined for this study obeys the unit normal distribution, and the only controlling parameter is p_{RMS}. It should be remembered that not all jet-noise signals will obey this distribution. Some high-speed jets (e.g., ones that exhibit crackle) have amplitude distributions that are not symmetric about zero (e.g., [32]). Although not shown, no such asymmetry was found in any of the signals examined in this study.

Looking at the peak amplitudes, the analysis becomes a bit more complicated. The PDF of the peak amplitudes for all 21 cases at 30 deg (all the cases used in Fig. 4a) is shown in Fig. 5. Although good collapse is once again achieved, the distribution is not quite the unit normal. The transformation to a log-parabolic space, shown in Fig. 5b, confirms that the distribution of the event amplitudes is indeed well described by a normal distribution by virtue of the linearity of the distribution in this space. As should be expected, the

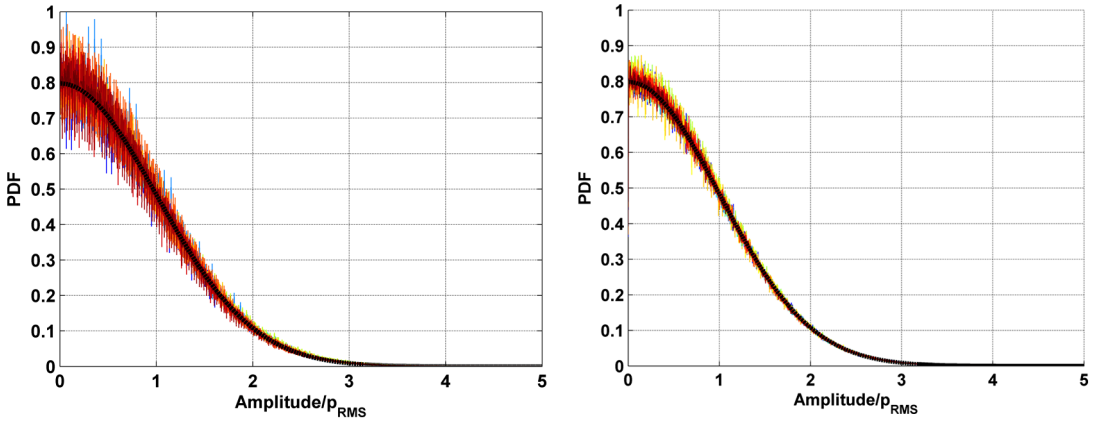

a) Total signal amplitude distribution for all 21 cases at $\phi = 30^\circ$

b) Total signal amplitude distribution for allpolar angles in Case 5 ($D = 2.54$ cm, TTR = 1.00, $M_a = 0.9$)

Fig. 4 PDF of the amplitude of unaltered original signals normalized by p_{RMS} for a given signal.

distribution is sharply cut off at $1.5p_{\mathrm{RMS}}$ as a consequence of the event definition. The best fit curve, however, is a normal distribution with a standard deviation of $\sigma = 1.2$. If the PDF was determined from a signal that was simply truncated below $1.5p_{\mathrm{RMS}}$, it would be equivalent to truncating the distribution in Fig. 4a at 1.5 and renormalizing for unit area. The departure from the unit normal can be explained by two factors. First, this distribution examines only the peak amplitudes. Points that would contribute to the distribution (i.e., all points in the signal above $1.5p_{\mathrm{RMS}}$) are discarded unless they happen to be a peak. This is effectively like turning the gradual rise and fall of a peak into a delta function. The result of this process is that the distribution becomes slightly skewed toward values that are more likely to be peaks (i.e., larger values). Second, when two initially distinct peaks are determined to be overlapping, the two peaks are classified as a single event, and only the larger peak is kept (see data-extraction step 4 in Sec. III). This also results in a preferential selection of larger amplitudes. The final result is that the distribution of peak amplitudes for all signals examined in this study (i.e., every polar angle for all cases) is described by the normal distribution with a σ of 1.2 and the value of p_{RMS} for a given signal.

B. Width Distributions

As discussed in Sec. III, the event width δt_i is defined as the full width at half-maximum (FWHM). The distribution of event widths provides information about the characteristic time scale of the flow-field phenomenon that produced the acoustic event.

1. ϕ Equal to Thirty Degrees

The distributions of event widths for the various cases at the 30 deg microphone are shown in Fig. 6. In the unheated-jet cases, the various velocities (acoustic Mach numbers) group very tightly according to jet diameter (Fig. 6a), indicating that the jet diameter is a representative length scale of the events, but that the acoustic Mach number is not a representative velocity scale. However, upon close inspection (see Table 2), a trend with acoustic Mach number is detectable, but it is a weak dependence when compared to diameter and temperature variations. Given the very weak dependence on acoustic Mach number and thus jet velocity, it can also be concluded that the convective velocity would not be a proper scaling. In the case of heated jets, the acoustic Mach number dependence becomes somewhat more significant. In the elevated-temperature cases, however, there is a clear trend toward larger values with increasing temperature, especially for the lower velocity. This suggests that something in the noise producing dynamics changes at elevated temperatures and this new behavior is much more sensitive to the jet velocity. The $M_a = 0.9$ and TTR $= 1.0$ cases for each of the three diameters are rescaled into inverse Helmholtz number (τ_∞) and plotted in Fig. 6b. Although this scaling does bring the distributions closer together, it does not collapse them. This result suggests that the dynamical length scale does not increase one-to-one with the jet diameter (it suggests that it increases more slowly), but it is not appropriate to draw a conclusion about this with only three points to make a trend line.

Koenig et al. [27] observe these same trends by looking at spectral collapse. They note that Helmholtz scaling does a better job of collapsing the spectra at 30 deg for unheated jets of a single diameter, whereas Strouhal number scaling does a better job for collapsing the hot jet cases. Their work to date does not include a parametric evaluation of jet diameter effects. It can be seen from Fig. 6 that Helmholtz scaling (lacking U_j dependence) would be a superior choice to Strouhal number scaling for the event widths in unheated

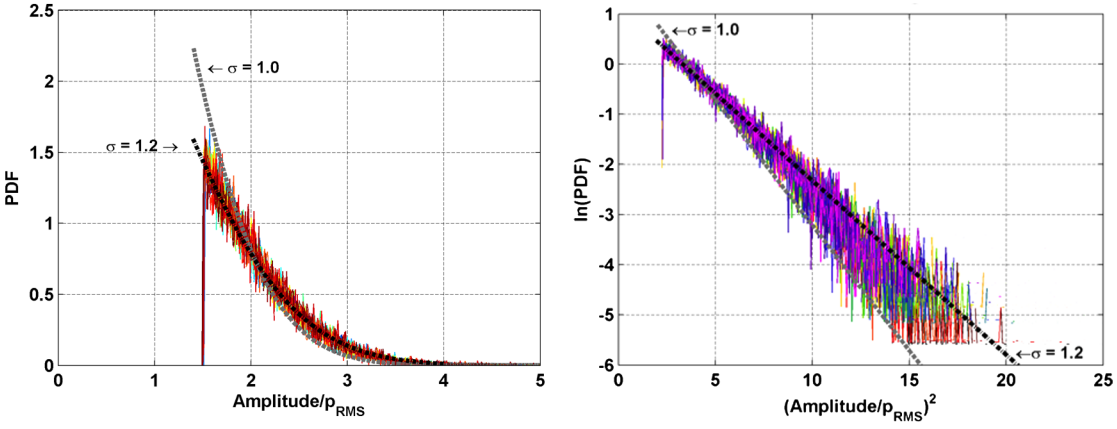

a) PDF of peak amplitudes

b) Log-parabolic plot of PDF of peak amplitudes

Fig. 5 PDF of peak amplitudes for all cases at $\phi = 30$ deg.

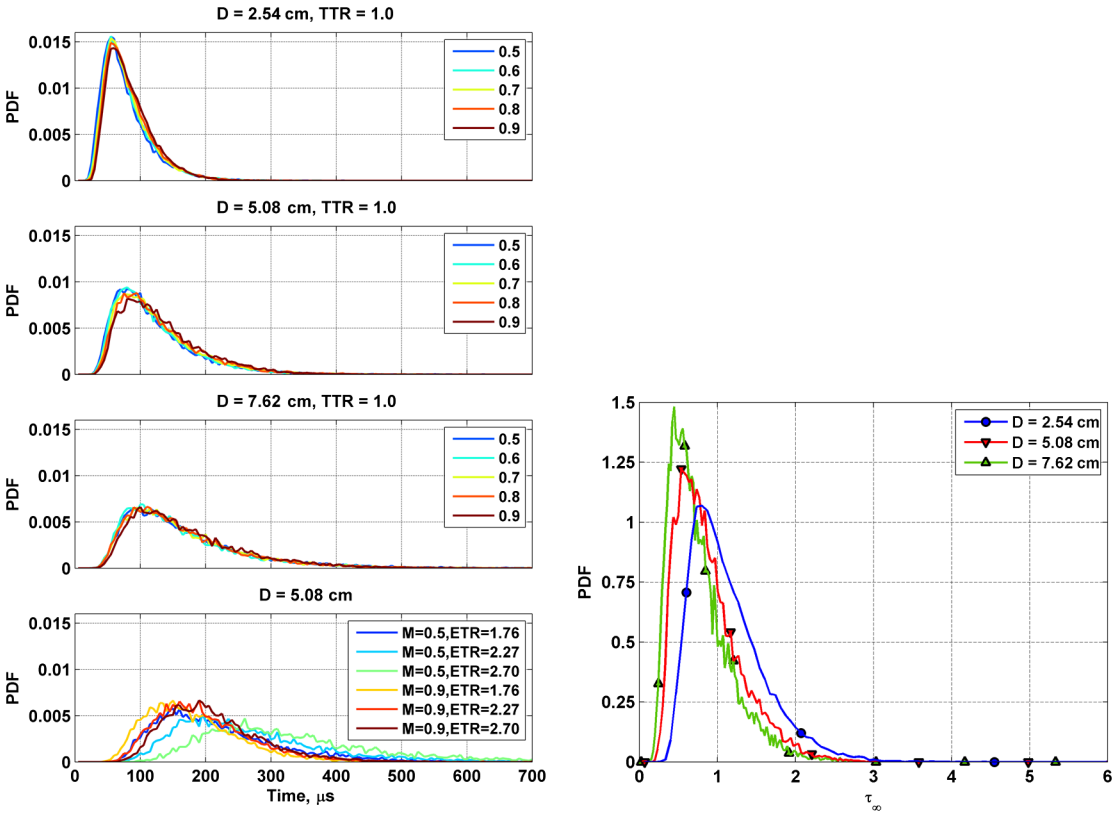

a) PDF with time abscissa

b) PDF with scaled time (τ_∞) for M_a = 0.9 and TTR = 1.0

Fig. 6 Distribution of event widths for all cases at $\phi = 30$ deg.

jets, and that Strouhal number scaling is also inappropriate for the hot jets. In a related work, Cavalieri et al. [33] propose that the superiority of Helmholtz scaling in the unheated jets is related to the noncompactness of the source associated with the azimuthally symmetric portion of the acoustic signal radiating to the aft angles. They extend this idea to suggest that the source becomes more compact at elevated temperatures due to the disparity in the speed of sound between the jet core and the ambient. Cavalieri et al. [33] also note that, although the axisymmetric mode scales with Helmholtz number, the first helical mode scales with Strouhal number, and they observe that the axisymmetric mode is only dominant at the aft angles. An alternate possibility is that the hot jet introduces additional compressibility and/or viscosity considerations. The work of Kambe [34] on vortex collisions showed that the viscous dominated aspects of the collision process are significant to the noise produced in the collision.

The distributions of event widths are fit with the gamma distribution, and it is found that it is indeed a good fit (as expected, given that the gamma distribution describes randomly distributed positive quantities); the fit parameters are enumerated in Table 2. Additionally, in Table 2, the mean event width $\overline{\delta t}$ for the various cases is enumerated, and the scaled values for both τ_j and τ_∞ are calculated. Although not tabulated, the product of ℓ and ξ, the mean of the gamma distribution, is a reasonably good match to the mean of the data (the maximum discrepancy is 10%). This agreement supports the statement that the gamma distribution is a good fit to the data. Detailed inspection of the distribution and best fit curves (not shown) confirms that these distributions are well described by the gamma distribution; this is an expected result because the gamma distribution describes randomly distributed positive numbers. It can be seen from the values in Table 2 that neither a Strouhal number nor a Helmholtz-type scaling properly collapses the data. Looking at the general trend in the average width versus jet diameter or temperature for a given acoustic Mach number, the average event width appears to be scaling in a uniform manner, but conclusions should not be drawn until the polar-angle dependence is examined (Sec. VI.D).

To examine the relationship between the distributions and the trends in the mean width, the distribution widths were scaled by their respective means, and the PDFs for all 21 cases are shown in Fig. 7. Additionally, a gamma distribution curve based on the averaged gamma parameters ($\ell = 5.72$ and $\xi = 0.17$) is shown as a black dashed line. It should be noted that ξ should be nondimensionalized by the mean event width for a given case before averaging. Although the collapse is not quite as good as the amplitude distributions, it is still sufficient to say that the mean event width is the controlling

Table 2 Various calculated quantities for the event width distributions at $\phi = 30$ deg

	Jet parameters			Gamma parameters			Mean δt	
Case number	D, cm	M_a	ETR	ℓ	ξ, μs	Time, μs	τ_j	τ_∞
1	2.54	0.5	~1	5.75	12.36	77.7	0.51	1.02
2	2.54	0.6	~1	6.16	11.94	80.0	0.63	1.05
3	2.54	0.7	~1	6.18	12.07	80.4	0.75	1.06
4	2.54	0.8	~1	6.49	11.82	82.6	0.88	1.09
5	2.54	0.9	~1	6.50	12.25	84.4	1.01	1.11
6	5.08	0.5	~1	4.86	22.16	119.2	0.39	0.78
7	5.08	0.6	~1	4.95	22.13	119.7	0.47	0.79
8	5.08	0.7	~1	4.99	22.91	124.1	0.57	0.82
9	5.08	0.8	~1	4.99	23.54	127.4	0.67	0.84
10	5.08	0.9	~1	5.00	24.82	132.3	0.78	0.87
11	7.62	0.5	~1	4.18	35.97	167.9	0.37	0.74
12	7.62	0.6	~1	4.33	33.31	161.0	0.42	0.71
13	7.62	0.7	~1	4.27	35.42	165.4	0.51	0.72
14	7.62	0.8	~1	4.37	34.30	163.3	0.57	0.72
15	7.62	0.9	~1	4.54	34.68	170.3	0.67	0.75
16	5.08	0.5	1.76	5.89	34.72	218.6	0.72	1.44
17	5.08	0.9	1.76	6.34	27.71	180.5	1.07	1.19
18	5.08	0.5	2.27	6.61	37.58	263.7	0.87	1.73
19	5.08	0.9	2.27	7.66	25.20	198.8	1.18	1.31
20	5.08	0.5	2.70	7.19	43.52	337.5	1.11	2.22
21	5.08	0.9	2.70	8.83	23.28	211.8	1.26	1.39

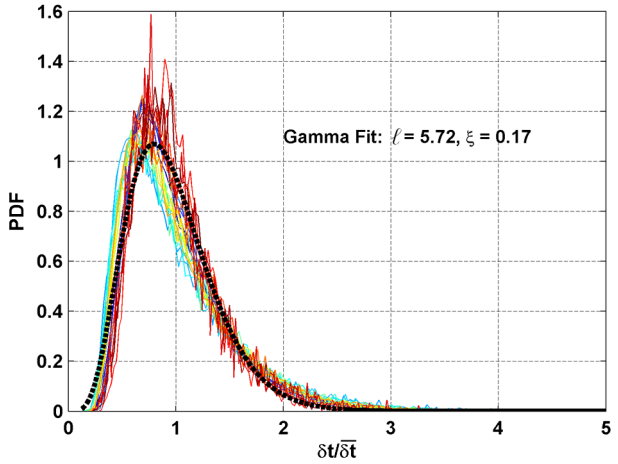

Fig. 7 Distribution of event widths normalized by their respective means for all 21 cases at $\phi = 30$ deg.

parameter in the distribution of event widths. Once the mean value is known, the entire distribution can be reasonably well predicted based on universal values for $\ell \approx 5.72$ and $\xi \approx 0.17$.

There are several conclusions to draw from these results:

1) The mechanism that produces these noise events does not seem to correlate with the jet velocity, but it does correlate with diameter and temperature. Furthermore, the changes in the distributions with jet diameter do not scale one-to-one with the jet diameter.

2) The agreement of the data with a gamma distribution indicates that the lifetimes or time scales of these events are uncorrelated (i.e., independent from one another). This implies that the source mechanism of these events is sufficiently independent from one event to the next to make it unique.

3) There exists only one controlling parameter in the distribution (in this case, the mean width). Once that parameter is known, the entire distribution can be closely approximated, along with the universal values of ℓ and ξ.

2. *Sideline and Upstream Angles*

The distributions of the event widths at the sideline and upstream angles are much more difficult to interpret. Per the definition of the event width, the minimum allowed event width is 10 μs. Although not shown, the peak of the distribution, regardless of operating conditions, occurs at a very short time, and it is also fairly constant. The peaks in all of the cases are separated by no more than four data points. This confirms the discussion in Sec. V that the essential problem is that the events at the sideline and upstream angles based on the definition chosen in this paper are rapid oscillations whose true characteristics are at least partially obscured by the sampling rate of the data. Because it has been established that the event definition and analysis process cannot provide a description of sideline and upstream noise that is not contaminated by the sampling rate of the data, further analysis of these radiation directions will be more restricted.

3. *Joint Probability Density Function: Amplitude and Width, ϕ Equal to Thirty Degrees*

To explore the relationship between the amplitude and the width of the events, the joint PDF of the two variables is calculated for the 30 deg data. The distributions are normalized so that there is unit volume under the surface. Based on the scaling characteristics determined in Secs. VI.A and VI.B, the distributions are presented with the event widths δt normalized by the mean event width and binned at the resolution of the data (5 μs). The peak amplitude p_{peak} is normalized by the RMS pressure, and the data are divided into 70 bins between $1.5p_{\text{RMS}}$ and $3.5p_{\text{RMS}}$.

If the two variables are statistically independent, the combination of a given amplitude and width would simply be the product of the distributions for the two variables. Another possibility is that the width and amplitude are related by some geometric relationship. A simple example of such a relationship is that of the width and height of an isosceles triangle with a constant spreading angle. In this simple example, fractional changes in width are equal to fractional changes in height (i.e., if the height doubles, the width doubles).

The joint PDFs for several cases are shown in Fig. 8. Figures 8a–8c show the variation with diameter, Figs. 8d–8f show the variation with acoustic Mach number, Figs. 8g–8i show the variation with ETR at $M_a = 0.5$, and Figs. 8j–8l shown the variation with ETR at $M_a = 0.9$. There is very little change in the distribution with diameter; the peak of the distribution decreases slightly with increasing diameter. There is essentially no change in the distribution width acoustic Mach number; consistent with the conclusions from Sec. VI.B.1. Heating does produce noticeable changes. In both acoustic Mach numbers, increasing the temperature causes the distribution to elongate in the p_{peak} direction (i.e., for a given width, larger-amplitude events become more probable with increasing temperature) while the width dimension is relatively fixed. The elongation is not extreme, but it is significant.

It is immediately clear that the width and the amplitude are not independent, but determining the nature of the dependence is considerably more difficult. The dashed line is the doubling line (i.e., the width doubles when the amplitude doubles) that passes through the peak of the distribution. For any given amplitude, the peak width follows the doubling line quite well across all of the cases. If the width and amplitude were deterministically linked and all events had the same spreading angle, then the distribution should tightly follow the dashed line on the figures. Because, however, there is no reasonable expectation (as seen from the broad variation in widths for any given amplitude) for all events (even of a single amplitude) to have the same spreading angle, it is concluded that the two quantities are correlated, but not deterministically. The consistent match between the doubling line and the peak of the distribution suggests that there is a characteristic shape to the events that scales depending on the amount of energy in the event. One other conclusion is that the elongation of the distribution along the doubling line with heating indicates that heating results in a greater proportion of large-amplitude large-width events.

C. Intermittence Distributions: Thirty Degrees

The last characteristic of the noise event needed to complete the picture is the time between the events (the intermittence). It should be noted that this intermittence is not related to the fluid dynamics concept of turbulence "intermittency" [35]. Based on the preceding discussion, only 30 deg is analyzed as the representative sample of aft angle noise. Generally, the Nth-order intermittence can be written as

$$\Delta T_i^{(N)} = T_i - T_{i-N} \tag{3}$$

where T_i is the temporal location of the ith event peak, as discussed in Sec. III. The distribution of the Nth-order intermittence is then found by calculating the histogram of the set $\{\Delta T_i^{(N)}\}_i$. As can be seen in the sample signals plotted in Fig. 2, the true nature of the large-amplitude signal fluctuations (beyond the $1.5p_{\text{RMS}}$ threshold) often includes at least one positive fluctuation and one negative fluctuation consecutively. Because these fluctuations are identified as distinct events, an indiscriminate calculation of the intermittence distribution would likely be skewed by the statistics regarding the spacing of these consecutive positive-to-negative swings. This positive-to-negative interval information is characterized by the event widths, and so it is redundant to include it here. The simplest solution to this issue is to look at peaks of one sign only, and this is the method that will be used. The results from looking at only positive peaks and then only negative peaks can be averaged together to conserve the statistical population size of the analysis. Because at least some events consist of multiple positive and negative swings, it is also prudent to average over several orders of intermittence. Based on the assumption that the $N = 2$ distribution should have a characteristic value approximately twice that of the $N = 1$ distribution, the average of M orders of the Nth-order distribution $H_j^{(N)}$ can be calculated as

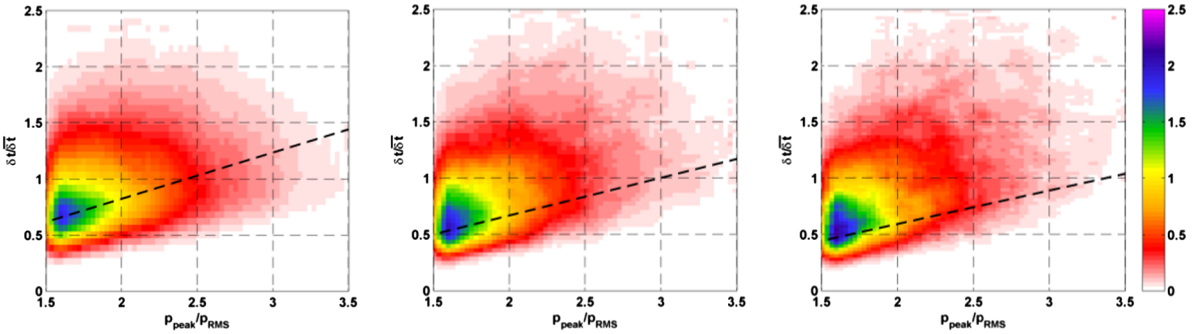

a) $M_a = 0.9$, $D = 2.54$ cm Case 5 b) $M_a = 0.9$, $D = 5.08$ cm Case 10 c) $M_a = 0.9$, $D = 7.62$ cm Case 15

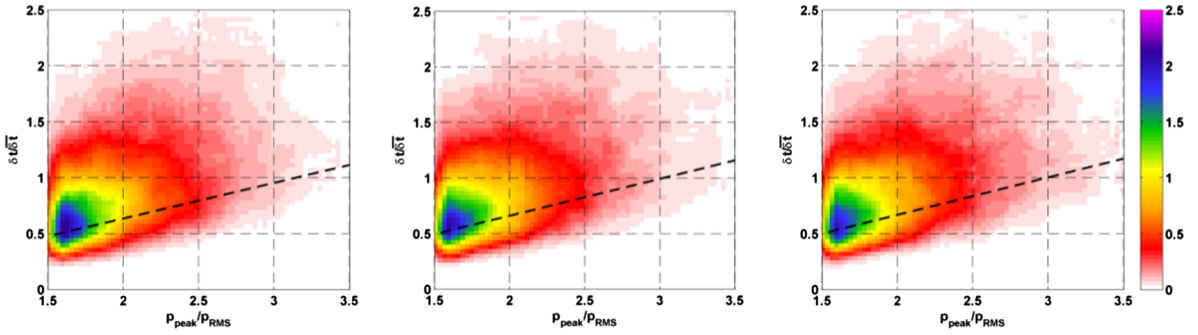

d) $D = 5.08$ cm, $M_a = 0.5$ Case 6 e) $D = 5.08$ cm, $M_a = 0.7$ Case 8 f) $D = 5.08$ cm, $M_a = 0.9$ Case 10

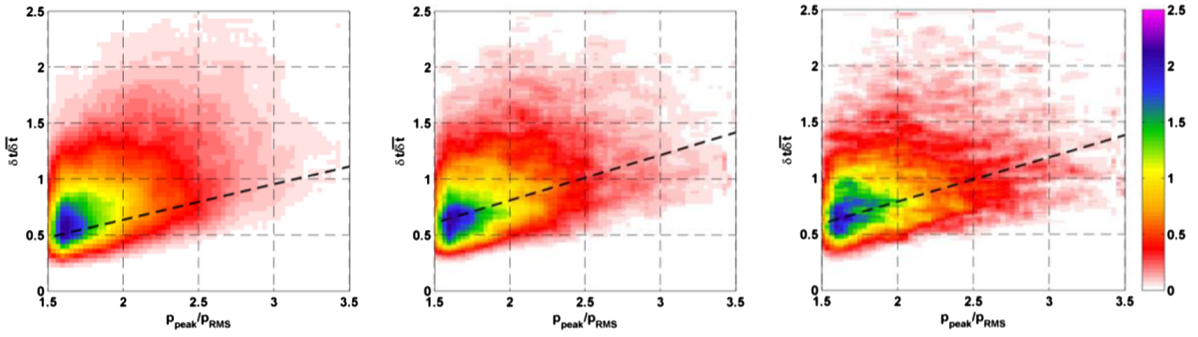

g) ETR = 0.85, $M_a = 0.5$ Case 6 h) ETR = 1.76, $M_a = 0.5$ Case 16 i) ETR = 2.70, $M_a = 0.5$ Case 20

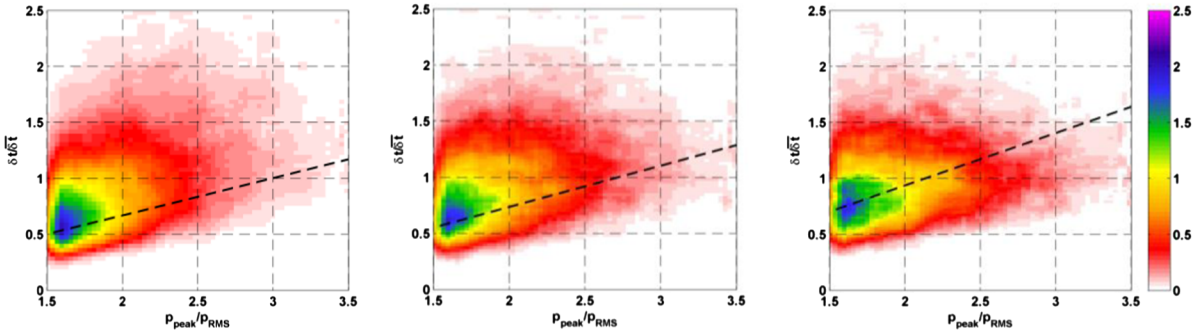

j) ETR = 0.85, $M_a = 0.9$ Case 10 k) ETR = 1.76, $M_a = 0.9$ Case 17 l) ETR = 2.70, $M_a = 0.9$ Case 21

Fig. 8 Joint PDFs of event amplitude and width for several operating conditions at $\phi = 30$ deg.

$$\Upsilon_j = \frac{1}{M}\sum_{N=1}^{M} NH_{jN}^{(N)} \tag{4}$$

where j denotes the jth bin of the distribution. The Nth-order distribution is downsampled by a factor of N (indicated by the subscript jN) and scaled by a factor of N to conserve the area under the curve. The downsampled and scaled distributions can then be point-by-point averaged.

The distributions of event intermittence are shown for the 30 deg data in Fig. 9. It is clear that, apart from the time scale, the distributions of event intermittence behave very similarly to the event width. The small secondary peak close to the origin is evidence of the peak-to-peak swing time scale already discussed. A relatively weak dependence on jet velocity for the unheated jets is observed, as are strong dependencies on jet diameter and temperature. In the hot jet cases, a velocity dependence is also present. Once again, the data lends itself to description by the gamma distribution. The best-fit gamma parameters as well as the mean event intermittence $\overline{\Delta T}$ are

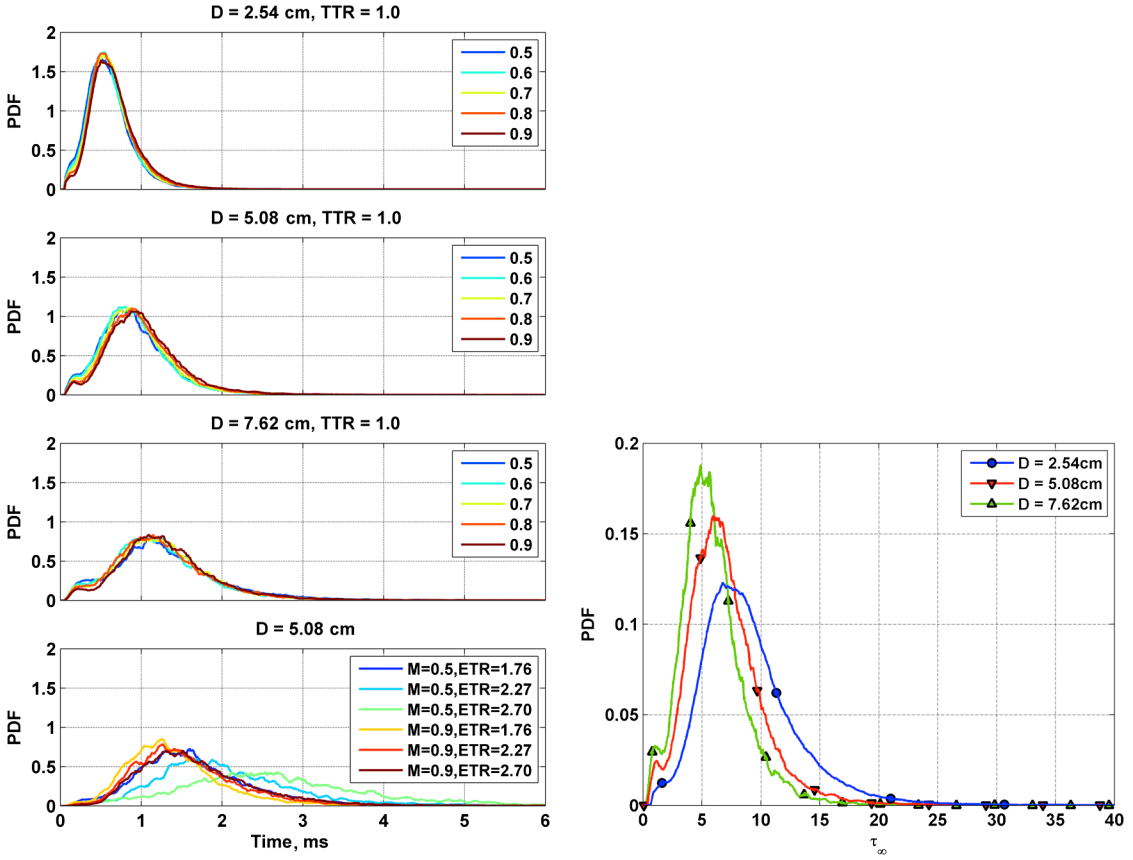

a) Unscaled distributions

b) PDF with scaled time (τ_∞) for M_a = 0.9 and TTR = 1.0

Fig. 9 Distribution of events intermittence for all cases at $\phi = 30$ deg.

listed in Table 3. The mean of the best fit gamma distribution matches the empirical mean reasonably well (maximum discrepancy is 4%), and a detailed examination of the best fit curves (not shown) shows that the data is indeed well described by the gamma distribution. The degree of similarity in the trends between event width and intermittence is actually quite high. If the ratio of the mean event width to the mean intermittence is calculated for all cases, the average and standard deviation of that set of ratios is $\overline{\delta t}/\overline{\Delta T} = 0.128 \pm 0.002$. This indicates that the mean intermittency of events and the mean lifetime of those events are strongly correlated. Additionally, the order of magnitude disparity in these quantities is in contravention to the sinusoidal behavior of typical wave-packet models.

Table 3 Various calculated quantities for the event intermittence distributions at $\phi = 30$ deg

	Jet parameters			Gamma parameters		Mean ΔT		
Case number	D, cm	M_a	ETR	ℓ	ξ, μs	Time, ms	St_D	He
1	2.54	0.5	~1	5.53	109.50	0.60	0.25	0.13
2	2.54	0.6	~1	5.99	102.71	0.61	0.20	0.12
3	2.54	0.7	~1	6.29	99.87	0.63	0.17	0.12
4	2.54	0.8	~1	6.60	95.92	0.65	0.15	0.12
5	2.54	0.9	~1	6.32	103.45	0.67	0.13	0.11
6	5.08	0.5	~1	5.08	185.42	0.92	0.33	0.17
7	5.08	0.6	~1	5.69	163.21	0.92	0.27	0.16
8	5.08	0.7	~1	6.04	159.12	0.95	0.23	0.16
9	5.08	0.8	~1	6.03	166.03	0.98	0.19	0.15
10	5.08	0.9	~1	6.34	163.43	1.05	0.16	0.15
11	7.62	0.5	~1	4.59	294.80	1.30	0.35	0.18
12	7.62	0.6	~1	5.18	244.33	1.24	0.31	0.18
13	7.62	0.7	~1	5.51	238.54	1.28	0.25	0.18
14	7.62	0.8	~1	5.41	236.62	1.27	0.22	0.18
15	7.62	0.9	~1	6.26	212.27	1.31	0.19	0.17
16	5.08	0.5	1.76	6.54	252.91	1.71	0.18	0.09
17	5.08	0.9	1.76	6.63	210.56	1.43	0.12	0.11
18	5.08	0.5	2.27	6.84	294.60	2.08	0.15	0.07
19	5.08	0.9	2.27	6.56	234.35	1.60	0.11	0.10
20	5.08	0.5	2.70	6.24	437.32	2.73	0.11	0.06
21	5.08	0.9	2.70	6.37	258.76	1.70	0.10	0.09

Following the same approach as in Sec. VI.B.1, the intermittence distributions of all 21 cases are scaled by their respective means and plotted in Fig. 10 along with a gamma distribution curve given by the average gamma parameters ($\ell = 6.0$ and $\xi = 0.17$). With the mean quantity scaled out, the distribution of the event intermittence is also seen to be universal and to be well predicted by a gamma distribution. These noise events are independent; that is, the occurrence of one event does not influence the occurrence of another. This conclusion was also reached by Guj et al. [21]. Again, these results are in contrast to typical wave-packet models that are based on a nearly sinusoidal ansatz. Last, there is only one controlling parameter on the distribution (the mean) and, once known, the entire distribution may be predicted. It is also worth noting that, in addition to the link between their mean values as already discussed, the distribution of event intermittence has very similar gamma parameters to the event width distribution.

As mentioned in Sec. II, Cavalieri et al. [33] noted that scaling the frequency axis into the Helmholtz number can achieve better spectral collapse than Strouhal number scaling for varying acoustic Mach number in an unheated jet. This implies that the spectral characteristics depend, at most, weakly on the jet velocity. Inspection of the 30 deg spectra on a Helmholtz number axis in Fig. 11 reveals a fairly constant value of the peak Helmholtz numbers irrespective of acoustic Mach number for the unheated jets. This is similar to the trends observed in the event intermittence as well as event widths. The amplitudes of the spectral peaks in Fig. 11 are artificially aligned. The collapse is quite similar to that observed in Cavalieri et al. [33]. This question of Helmholtz versus Strouhal number scaling has been a subject of much discussion (e.g., [36,37]). As can be seen in Fig. 11,

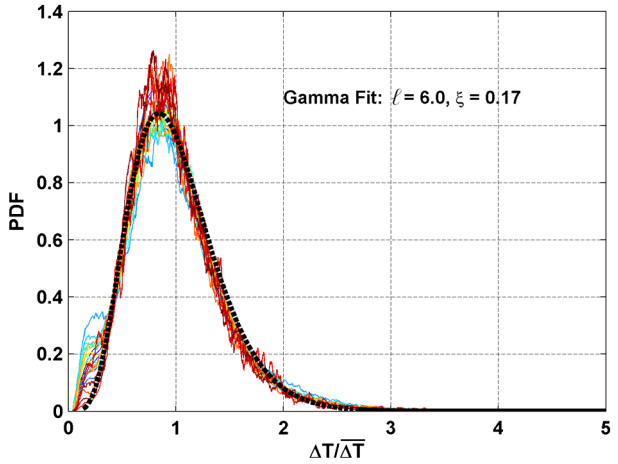

Fig. 10 Intermittence distributions normalized by their respective means for all 21 cases at $\phi = 30$ deg.

Helmholtz scaling does a good job of collapsing the portion of the spectrum to the right of the spectral peak, but it does not do a good job with the portion to the left of the spectral peak. A similar result has been observed before [36] but was usually associated with 1/3-octave spectral analysis compared to narrowband analysis, which is clearly not the case in the current work. Settling this debate is beyond the scope of this work, but the statistical analysis of noise events supports the idea that Helmholtz scaling is a superior descriptor of the underlying dynamics, at least for unheated jets.

The value of the mean intermittence, converted into Helmholtz number, is marked with triangles in Fig. 11. The mean intermittence is reasonably well correlated with the peak in the spectrum. Given the strong correlation between the mean event width and mean intermittence, however, either one could be the causal parameter of the spectral peak. The prediction is not quite as good for the low-speed 7.62 cm cases. This may be due to the properties of the anechoic chamber combined with the frequencies of the jet. As discussed in Sec. IV, the anechoic chamber is effective down to about 200 Hz. The peak frequencies of the 7.62 cm jet are close to the limits of the chamber, so it is possible that the results are being skewed by reflections. In the elevated-temperature cases, prediction is reasonably good for the low-speed cases, but it is a bit low for the high-speed cases. It is possible that combustor noise is skewing these results. Given the additional complexities of the hot jet cases, the agreement is decent.

D. Directivity of Mean Event Width

Analysis of the 30 deg microphone signals has shown that there are a few important variables governing these noise events. With that information, more polar angles are examined. The mean width $\overline{\delta t}$ directivity for the five acoustic Mach numbers in the unheated jet is shown in Fig. 12a. The first thing to note is that there is very little variation in this directivity for the different acoustic Mach numbers. Apart from some subtle trends with velocity that have already been discussed in more detail in Sec. VI.B, these directivity patterns are essentially identical. There is some apparent variation in the upstream angles, but as already discussed, the information from these directions is of limited use due to the nature of the signals. There is also more variation in the 15 deg microphone, but that might be expected given the close proximity to the jet plume. Another important observation is that, beyond 55 deg, the mean width becomes constant. This indicates (as can be confirmed by examination of the spectra) that the noise radiated to angles of 60 deg and higher has a similar nature. It is also found that the gamma parameters that

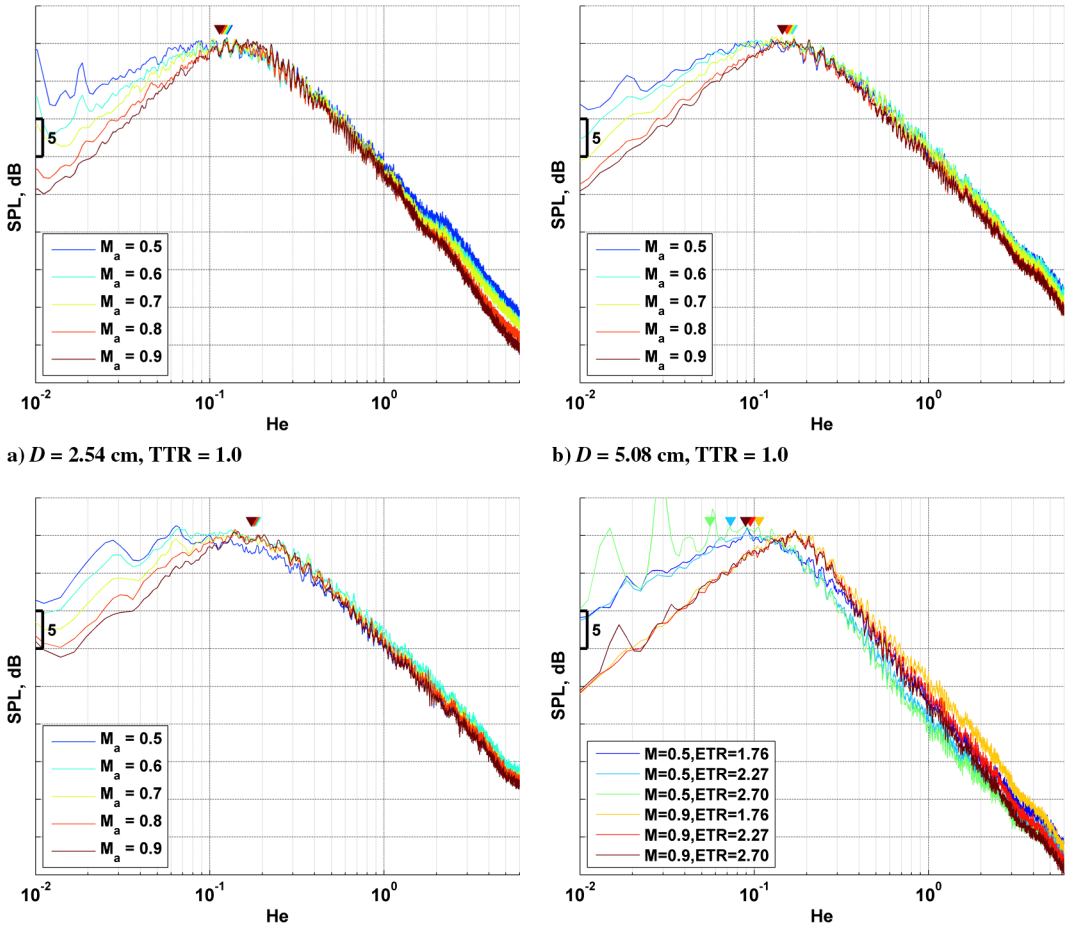

a) D = 2.54 cm, TTR = 1.0

b) D = 5.08 cm, TTR = 1.0

c) D = 7.62, TTR = 1.0

d) D = 5.08 cm, elevated temperatures

Fig. 11 Spectra at $\phi = 30$ deg showing the predictive capability of the mean intermittence.

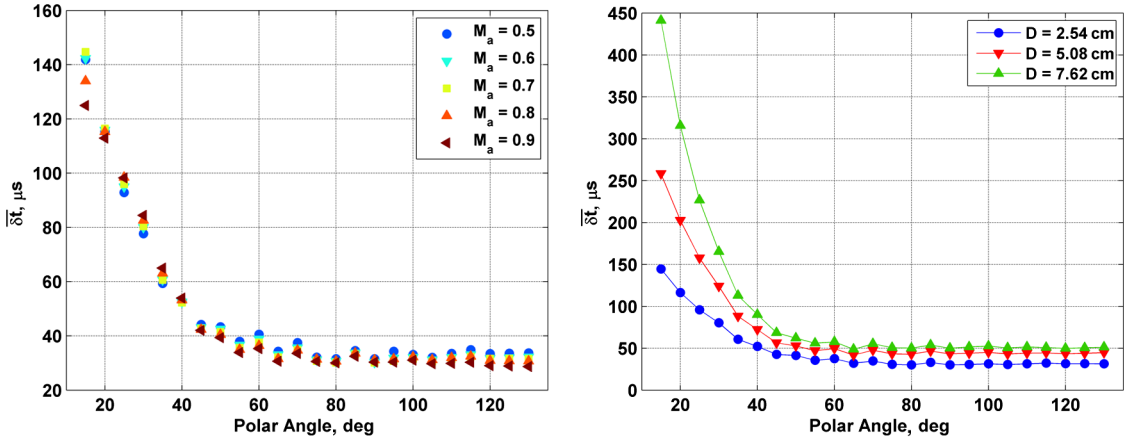

a) Various Mach numbers for $D = 2.54$ cm & TTR = 1.0

b) Various diameters for $M_a = 0.7$ & TTR = 1.0

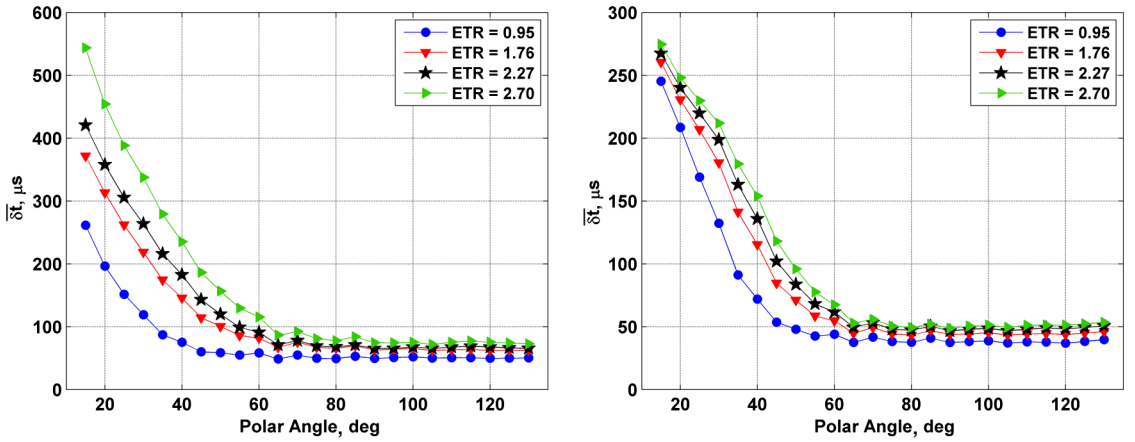

c) Various exit temperature ratios for $D = 5.08$ cm & $M_a = 0.5$

d) Various exit temperature ratios for $D = 5.08$ cm & $M_a = 0.9$

Fig. 12 Directivity patterns for mean event width.

describe the distributions follow similar trends with polar angle (not shown). The shape parameter ℓ changes much less than the rate parameter ξ. The shape of the gamma distribution changes gradually with polar angle.

The directivity of the mean width for the three jet diameters is shown for the unheated jet and the middle acoustic Mach number ($M_a = 0.7$) in Fig. 12b. Although the sideline and upstream angles change very little, it is clear that the mean width has a coupled dependence on the jet diameter and polar angle for the aft angle noise. The dependence on the jet temperature is also complex (Figs. 12c and 12d). Again, there is very little change in the sideline and upstream angles. The mean width in the transition angles ($\phi = 40$ to 60 deg) changes more rapidly as the jet gets hotter. The aft angles ($\phi = 15$ to 35 deg), however, have a fairly constant slope, with their absolute values being dictated by the changes in the transition angles. Last, it is seen that a larger jet velocity significantly suppresses these trends with temperature. It is not clear at this time how to construct an appropriate scaling scheme to account for these trends. It is likely that a much more extensive data set would be required to understand it fully.

The mean width $\overline{\delta t}$ and intermittence $\overline{\Delta T}$ are shown versus polar angle for case 5 ($D = 2.54$ cm, $M_a = 0.9$, TTR = 1.0) in Fig. 13, where the mean intermittence has been scaled by 0.128, based on the conclusion reached in Sec. VI.C. Case 5 was chosen as a representative sample. This shows that there is a strong and consistent relationship between the mean event width and intermittence regardless of polar angle, further supporting the idea that the two are dynamically linked.

Returning to the comparison of the mean intermittence (and the mean width by way of the correlation between these two quantities) to the spectral peak (Fig. 11), it is found that, in terms of Helmholtz number, the spectral peak frequency at the aft angles is fairly constant for a given jet diameter and polar angle in the unheated jet. In contrast, the spectral peak Strouhal number for angles above about 50 deg is reasonably constant. Although there are not any additional figures (in the interest of brevity) showing direct comparisons for polar angles other than 30 deg (see Fig. 11), the mean intermittence is a good match to the spectral peak for the aft angles. On the range $\phi = 15$ to 40 deg, the prediction is generally quite good. For higher polar angles, the peak frequency is consistently overpredicted, but as

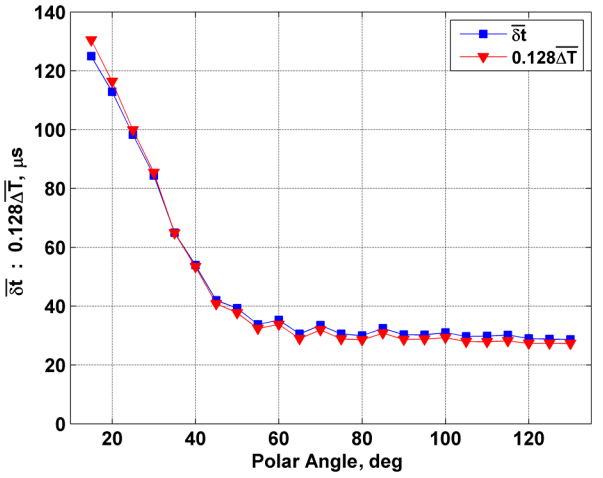

Fig. 13 Directivity pattern of mean width and intermittence for case 5 ($D = 2.54$ cm, $M_a = 0.9$, and TTR = 1.0).

already discussed, this analysis does not expect to correctly predict the properties of radiation to the sideline and upstream angles.

E. Summary of Statistics Results

The statistical analysis of noise events has yielded a large number of observations and conclusions. The summary of those observations is as follows:

1) The far-field acoustic signal radiating to the aft polar angles can be well represented by intermittent bursts of noise. In this study, these bursts are defined as regions of the signal with amplitudes larger than $1.5p_{\mathrm{RMS}}$.

2) The analysis of events in the sideline and upstream directions was limited by the sampling rate of the signal, and it is therefore possible that noise events are present in the sideline and upstream angles but are very short-lived events and so could not be properly analyzed in this study.

3) Using a model with three important parameters in the acoustic signal (peak amplitude, event width, and the time between events), the following are educed from the analysis:

a) The distribution of peak amplitudes obeys a universal normal distribution across all polar angles and operating conditions once scaled by p_{RMS} of the original signal. The normal distribution ($\sigma = 1.2$) is close to the unit normal but slightly skewed toward larger amplitudes, as already discussed.

b) The distribution of event widths (looking only at the aft polar angles) obeys a universal gamma distribution for all cases at a given polar angle once scaled by the mean event width ($\overline{\delta t}$). There are small variations in the gamma parameters with polar angle, but the distributions are reasonably well described by a single universal distribution for all angles below about $\phi = 50$ deg. The fact that a gamma distribution accurately describes the event widths implies that the width of one event has no correlation to the width of other events; this result also implies that the sources of noise events are also independent.

c) The joint probability density functions of event width and amplitude show that there is a link between event amplitude and width that can be partially described by a simple geometric scaling.

d) The distribution of event intermittence has the same characteristics as the event width once scaled by the mean intermittence $\overline{\Delta T}$. This implies that the occurrence of one event is not correlated to the occurrence of preceding or subsequent events. It is also found that the universal distribution that describes the event intermittence is very similar to the distribution of the event width (gamma parameters $\ell \approx 6.0$ and $\xi = 0.17$).

e) There is a consistent relationship between the mean event width and the mean intermittence $\overline{\delta t}/\overline{\Delta T} = 0.128$. This implies a strong link between the governing dynamics controlling these two quantities.

4) Based on these observations, the entire signal for noise radiated to the aft angles can be reasonably well predicted in a statistical sense with knowledge of three quantities (p_{RMS}, $\overline{\delta t}$, and $\overline{\Delta T}$) along with the $\sigma = 1.2$ normal distribution and the gamma distribution ($\ell \approx 6.0$ and $\xi = 0.17$). It is actually possible to eliminate one or other of the mean quantities if the relationship in point 3e ($\overline{\delta t}/\overline{\Delta t} = 0.128$) is used.

5) The mean width and intermittence are fairly insensitive to changes in the jet velocity in an unheated jet, but they are significantly dependent on diameter and jet temperature. In the hot jet, there is also velocity dependence.

6) Directivity analysis of the mean quantities confirms the dependencies already discussed but also shows that the polar-angle dependence is intertwined with the diameter and temperature dependencies.

It is important to note that using the mean value of the distributions is a convenient scaling; it would work equally well to use the peak of the distribution or any other descriptive quantity of the distribution.

VII. Implications for Noise Sources

The most important result in terms of implications for existing noise-source models is that there are essential dynamics missing from the current models. Currently, the best models for the low-angle jet noise are noncompact source models based on wave-packets (e.g., [19,38]). As discussed in Sec. II, these wave-packets typically model a noise source as consisting of a simple harmonic travelling wave and some sort of envelope function (often a Gaussian). The assumption that linear superposition is valid (for both the source field and the resulting acoustic field) is then used to create complexity in the acoustic field. Although it may be mathematically possible to produce the rich behavior (described by the present statistical analysis) using this approach, the validity of linear superposition for the source field is tenuous. Furthermore, the rich behavior can only be accurately constructed by solving the adjoint problem using a known acoustic field. A model that overtly contained the key features identified by statistical analysis presented here would likely be a better physical description of the dynamics, at the cost of increased complexity compared to current models. Although these wave-packet models show good agreement with the directivity patterns of the overall sound signal, they do not include (at least in any direction fashion) a number of the features revealed by the current statistical analysis. If the wave-packet model is discussed in terms of any one frequency, the following issues are observed:

1) Noise events are only quasi-periodic at best, but the wave-packet model predicts a purely periodic signal.

2) The event width and intermittence are correlated, but not in a way that would be well represented by the simple harmonic wave used in a wave-packet.

3) The event width and intermittence have directivity patterns that have no direct representation in the wave-packet model.

The existing models should be examined to shed light on the best way to incorporate the dynamics revealed by the present statistical analysis.

VIII. Conclusions

Following on the previous works showing that the far-field jet noise has significant intermittent aspects, the present work hypothesized that these intermittent events are the dominant feature of jet noise. A definition and method of detection for noise events was devised and implemented. Using a large experimental database of acoustically subsonic jets with different velocities, diameters, and temperatures, these events were extracted from the noise signals. It was shown that a signal containing only these events retains all of the important aspects of the acoustic spectrum for jet noise radiating to aft angles. It is therefore concluded that these intermittent events are the dominant feature of aft-angle jet noise.

The characteristics of these noise events were statistically analyzed. It was shown that these events are uncorrelated and that they can be statistically described in terms of three parameters (p_{RMS} of the original signal, the mean width of the events, and the mean time between events) and two universal statistical-distribution curves. It was found that this intermittent nature occurred most prominently in the aft angles and was not detectable for polar angles greater than about $\phi = 60$ deg, potentially due to their much shorter temporal scale and the resolution limits of the data-acquisition system. These parameters have strong dependencies on jet diameter and temperature. The parameters have a very weak dependence on jet velocity for unheated jets but have significant velocity dependence in hot jets. It was also found that there exists a strong correlation between the mean width and the mean intermittence of the events. The ratio of these two quantities is consistently 0.128. This disagrees with the sinusoidal behavior of typical wave-packet models. The mean frequency of events (and the mean event width by way of the previously stated correlation) was shown to be correlated with the spectral peak frequency. The relationship of the present analysis to existing wave-packet models was discussed. Although the results found in this work cannot pinpoint noise sources, this new information should help narrow the focus of future work in the pursuit of understanding jet noise.

Acknowledgments

The support of this research by the NASA Glenn Research Center with James Bridges and Cliff Brown and the U.S. Air Force Office of

Scientific Research with John Schmisseur is greatly appreciated. The authors also want to thank all of the Aero-Acoustic Propulsion Laboratory personnel for providing the data for this project.

References

[1] Lighthill, M. J., "On Sound Generated Aerodynamically. 1. General Theory," *Proceedings of the Royal Society Series A*, Vol. 211, No. 1107, 1952, pp. 564–587. doi:10.1098/rspa.1952.0060

[2] Jordan, P., and Gervais, Y., "Subsonic Jet Aeroacoustics: Associating Experiment, Modelling and Simulation," *Experiments in Fluids*, Vol. 44, No. 1, 2008, pp. 1–21. doi:10.1007/s00348-007-0395-y

[3] Tam, C. K. W., Golebiowski, M., and Seiner, J. M., "On the Two Components of Turbulent Mixing Noise from Supersonic Jets," *2nd AIAA and CEAS Aeroacoustics Conference*, AIAA Paper 1996-1716, May 1996.

[4] Viswanathan, K., "Scaling Laws and a Method for Identifying Components of Jet Noise," *AIAA Journal*, Vol. 44, No. 10, 2006, pp. 2274–2285. doi:10.2514/1.18486

[5] Cabana, M., Fortuné, V., and Jordan, P., "Identifying the Radiating Core of Lighthill's Source Term," *Theoretical and Computational Fluid Dynamics*, Vol. 22, No. 2, 2008, pp. 87–106. doi:10.1007/s00162-008-0075-4

[6] Hileman, J., Thurow, B., Caraballo, E., and Samimy, M., "Large-Scale Structure Evolution and Sound Emission in High-Speed Jets: Real-Time Visualization with Simultaneous Acoustic Measurements," *Journal of Fluid Mechanics*, Vol. 544, 2005, pp. 277–307. doi:10.1017/S002211200500666X

[7] Viswanathan, K., "Analysis of the Two Similarity Components of Turbulent Mixing Noise," *AIAA Journal*, Vol. 40, No. 9, 2002, pp. 1735–1744. doi:10.2514/2.1878

[8] Panda, J., Seasholtz, R. G., and Elam, K. A., "Investigation of Noise Sources in High-Speed Jets via Correlation Measurements," *Journal of Fluid Mechanics*, Vol. 537, 2005, pp. 349–385. doi:10.1017/S0022112005005148

[9] Bogey, C., and Bailly, C., "An Analysis of the Correlations Between the Turbulent Flow and the Sound Pressure Fields of Subsonic Jets," *Journal of Fluid Mechanics*, Vol. 583, 2007, pp. 71–97. doi:10.1017/S002211200700612X

[10] Ukeiley, L., Tinney, C. E., Mann, R., and Glauser, M., "Spatial Correlations in a Transonic Jet," *AIAA Journal*, Vol. 45, No. 6, 2007, pp. 1357–1369. doi:10.2514/1.26071

[11] Hileman, J., Thurow, B., and Samimy, M., "Development and Evaluation of a 3-D Microphone Array to Locate Individual Acoustic Sources in a High-Speed Jet," *Journal of Sound and Vibration*, Vol. 276, Nos. 3–5, 2004, pp. 649–669. doi:10.1016/j.jsv.2003.08.022

[12] Ffowcs Williams, J. E., "Aeroacoustics," *Annual Review of Fluid Mechanics*, Vol. 9, 1977, pp. 447–468. doi:10.1146/annurev.fl.09.010177.002311

[13] Tam, C. K. W., "Jet Noise: Since 1952," *Theoretical and Computational Fluid Dynamics*, Vol. 10, Nos. 1–4, 1998, pp. 393–405. doi:10.1007/s001620050072

[14] Crighton, D. G., "Jet Noise and the Effects of Jet Forcing," *Lecture Notes in Physics*, Vol. 136, 1981, pp. 340–362. doi:10.1007/3-540-10289-2

[15] Crighton, D. G., "Acoustics as a Branch of Fluid Mechanics," *Journal of Fluid Mechanics*, Vol. 106, 1981, pp. 261–298. doi:10.1017/S0022112081001602

[16] Kastner, J., Kim, J.-H., and Samimy, M., "A Study of the Correlation of Large-Scale Structure Dynamics and Far-Field Radiated Noise in an Excited Mach 0.9 Jet," *International Journal of Aeroacoustics*, Vol. 8, No. 3, 2009, pp. 231–259. doi:10.1260/147547208786940008

[17] Grassucci, D., Camussi, R., Kerhervé, F., Jordan, P., and Grizzi, S., "Using Wavelet Transforms and Linear Stochastic Estimation to Study Nearfield and Turbulent Velocity Signatures in Free Jets," *16th AIAA/CEAS Aeroacoustics Conference*, AIAA Paper 2010-3954, June 2010.

[18] Cavalieri, A. V. G., Jordan, P., Gervais, Y., Wei, M., and Freund, J. B., "Intermittent Sound Generation and Its Control in a Free-Shear Flow," *Physics of Fluids*, Vol. 22, No. 11, 2010, p. 115113. doi:10.1063/1.3517297

[19] Cavalieri, A. V. G., Jordan, P., Agarwal, A., and Gervais, Y., "Jittering Wave-Packet Models for Subsonic Jet Noise," *Journal of Sound and Vibration*, Vol. 330, Nos. 18–19, 2011, pp. 4474–4492. doi:10.1016/j.jsv.2011.04.007

[20] Koenig, M., Cavalieri, A., Jordan, P., Delville, J., Gervais, Y., Papamoschou, D., Samimy, M., and Lele, S., "Farfield Filtering and Source Imaging for the Study of Jet Noise," *16th AIAA/CEAS Aeroacoustics Conference*, AIAA Paper 2010-3779, June 2010.

[21] Guj, G., Carley, M., Camussi, R., and Ragni, A., "Acoustic Identification of Coherent Structures in a Turbulent Jet," *Journal of Sound and Vibration*, Vol. 259, No. 5, 2003, pp. 1037–1065. doi:10.1006/jsvi.2002.5130

[22] Juve, D., Sunyach, M., and Comte-Bellot, G., "Intermittency of the Noise Emission in Subsonic Cold Jets," *Journal of Sound and Vibration*, Vol. 71, No. 3, 1980, pp. 319–332. doi:10.1016/0022-460X(80)90416-2

[23] Low, K. R., Berger, Z. P., Lewalle, J., El-Hadidi, B., and Glauser, M. N., "Correlations and Wavelet Based Analysis of Near-Field and Far-Field Pressure of a Controlled High Speed Jet," *41st AIAA Fluid Dynamics Conference and Exhibit*, AIAA Paper 2011-4020, June 2011.

[24] Grizzi, S., and Camussi, R., "Wavelet Analysis of Near-Field Pressure Fluctuations Generated by a Subsonic Jet," *Journal of Fluid Mechanics*, Vol. 698, 2012, pp. 93–124. doi:10.1017/jfm.2012.64

[25] Wei, M., and Freund, J. B., "A Noise-Controlled Free Shear Flow," *Journal of Fluid Mechanics*, Vol. 546, 2006, pp. 123–152. doi:10.1017/S0022112005007093

[26] Kastner, J., Samimy, M., Hileman, J., and Freund, J. B., "Comparison of Noise Mechanisms in High and Low Reynolds Number High-Speed Jets," *AIAA Journal*, Vol. 44, No. 10, 2006, pp. 2251–2258. doi:10.2514/1.18384

[27] Koenig, M., Cavalieri, A. V. G., Jordan, P., Delville, J., Gervais, Y., and Papamoschou, D., "Farfield Filtering of Subsonic Jet Noise: Mach and Temperature Effects," *17th AIAA/CEAS Aeroacoustics Conference*, AIAA Paper 2011-2926, June 2011.

[28] Koenig, M., Cavalieri, A. V. G., Jordan, P., and Gervais, Y., "Intermittency of the Azimuthal Components of the Sound Radiated by Subsonic Jets," *17th AIAA/CEAS Aeroacoustics Conference*, AIAA Paper 2011-2746, June 2011.

[29] Tanna, H. K., "An Experimental Study of Jet Noise. Part 1. Turbulent Mixing Noise," *Journal of Sound and Vibration*, Vol. 50, No. 3, 1977, pp. 405–428. doi:10.1016/0022-460X(77)90493-X

[30] Brown, C. A., and Bridges, J., "Small Hot Jet Acoustic Rig Validation," NASA TR-2006-214234, 2006.

[31] Bridges, J., and Brown, C. A., "Validation of the Small Hot Jet Acoustic Rig for Aeroacoustic Research," *11th AIAA/CEAS Aeroacoustics Conference*, AIAA Paper 2005-2846, May 2005.

[32] Papamoschou, D., and Debiasi, M., "Directional Suppression of Noise from a High-Speed Jet," *AIAA Journal*, Vol. 39, No. 3, 2001, pp. 380–387. doi:10.2514/2.1345

[33] Cavalieri, A. V. G., Jordan, P., Colonius, T., and Gervais, Y., "Axisymmetric Superdirectivity in Subsonic Jets," *Journal of Fluid Mechanics*, Vol. 704, 2012, pp. 388–420. doi:10.1017/jfm.2012.247

[34] Kambe, T., "Influence of Viscosity on Aerodynamic Sound Emission in Free Space," *Journal of Sound and Vibration*, Vol. 95, No. 3, 1984, pp. 351–360. doi:10.1016/0022-460X(84)90674-6

[35] Pope, S. B., *Turbulent Flows*, Cambridge Univ. Press, Cambridge, England, U.K., 2000, pp. 167–173.

[36] Bogey, C., Barré, S., Fleury, V., Bailly, C., and Juvé, D., "Experimental Study of the Spectral Properties of Near-Field and Far-Field Jet Noise," *International Journal of Aeroacoustics*, Vol. 6, No. 2, 2007, pp. 73–92. doi:10.1260/147547207781041868

[37] Bogey, C., Bailly, C., and Juve, D., "Noise Investigation of a High Subsonic, Moderate Reynolds Number Jet Using a Compressible Large Eddy Simulation," *Theoretical and Computational Fluid Dynamics*, Vol. 16, No. 4, 2003, pp. 273–297. doi:10.1007/s00162-002-0079-4

[38] Papamoschou, D., "Wavepacket Modeling of the Jet Noise Source," *17th AIAA/CEAS Aeroacoustics Conference*, AIAA Paper 2011-2835, June 2011.

A. Lyrintzis
Associate Editor